Parallaxes of Southern Extremely Cool objects I: Targets, Proper motions and first results.

A.H. Andrei[1,2,3], R.L. Smart[2], J.L. Penna[1], V. A. d'Avila[1,4], B. Bucciarelli[2], J.I.B. Camargo[1], M. T. Crosta[2], M. Daprà[2], B. Goldman[5], H.R.A. Jones[6], M.G. Lattanzi[2], L. Nicastro[7], D.N. da Silva Neto[8] and R. Teixeira[9]

ABSTRACT

We present results from the PARallaxes of Southern Extremely Cool objects (PARSEC) program, an observational program begun in April 2007 to determine parallaxes for 122 L and 28 T southern hemisphere dwarfs using the Wide Field Imager on the ESO 2.2m telescope. The results presented here include parallaxes of 10 targets from observations over 18 months and a first version proper motion catalog.

The proper motions were obtained by combining PARSEC observations astrometrically reduced with respect to the Second US Naval Observatory CCD Astrograph Catalog, and the Two Micron All Sky Survey Point Source Catalogue. The resulting median proper motion precision is 5mas/yr for 195,700 sources. The 140 0.3deg^2 fields sample the southern hemisphere in an unbiased fashion with the exception of the galactic plane due to the small number of targets in that region. The proper motion distributions are shown to be statistically well behaved. External comparisons are also fully consistent. We will continue to update this catalog until the end of the program and we plan to improve it including also observations from the GSC2.3 database.

We present preliminary parallaxes with a 4.2 mas median precision for 10 brown dwarfs, 2 of which are within 10pc. These increase by 20% the present number of L dwarfs with published parallaxes. Of the 10 targets, 7 have been previously discussed in the literature: two were thought to be binary but the PARSEC observations show them to be single, one has been confirmed as a binary companion and another has been found to be part of a binary system, both of which will make good benchmark systems. These results confirm that the foreseen precision of PARSEC can be achieved and that the large field of view will allow us to identify wide binary systems.

Observations for the PARSEC program will end in early 2011 providing 3-4 years of coverage for all targets. The main expected outputs are: more than a 100% increase of the number of L dwarfs with parallaxes; to increment - in conjuction with published results - to at least 10 the number of objects per spectral subclass up to L9, and; to put sensible limits on the general binary fraction of brown dwarfs. We aim to contribute significantly to the understanding of the faint end of the H-R diagram and of the L/T transition region.

Subject headings: Astrometry – Stars: low-mass, fundamental parameters, distances, proper motions

[1]Observatório Nacional/MCT, R. Gal. José Cristino 77, CEP20921-400, RJ, Brasil.

[2] INAF/Osservatório Astronomico di Torino, Strada Osservatório 20, 10025 Pino Torinese, Italy

[3] Observatório do Valongo/UFRJ, Ladeira Pedro Antônio 43, CEP20080-090, RJ, Brasil

[4] UERJ, Faculdade de Oceanografia, R. São Francisco Xavier 524, CEP20550-900, RJ, Brasil

[5]Max Planck Institute for Astronomy, Koenigstuhl 17, D–69117 Heidelberg, Germany

[6] Centre for Astrophysics Research, Science and Technology Research Institute, University of Hertfordshire, Hatfield AL10 9AB

[7]INAF/Istituto di Astrofisica Spaziale e Fisica Cosmica, Bologna, Via Gobetti 101, 40129 Bologna, Italy

[8] Centro Universitário Estadual da Zona Oeste, Av. Manuel Caldeira de Alvarenga 1203, CEP23070-200, RJ,

1. Introduction

The first brown dwarf, GD 165B, was discovered in 1988 (Becklin & Zuckerman) but was not recognised as such until 1995 when Gl229B (Nakajima et al.) and other objects with the same characteristics were found. Rapidly many examples were discovered primarily in the large infrared surveys, i.e. the Two Micron All Sky Survey (2MASS, Skrutskie et al. 2006) and Deep Near-Infrared Survey (DENIS, Epchtein et al. 1999), and, the deep optical Sloan Digital Sky Survey (SDSS, York et al. 2000). It was soon realized that new spectral types, L and T, were needed (Kirkpatrick et al. 1999). Since then over 700 L/T dwarfs have been discovered (www.dwarfarchives.org 2/2010) by various authors and just recently a sample of 210 new L dwarfs from the SDSS was announced (Schmidt et al. 2010a). These objects have heralded a whole new sub-field of astronomy.

Interest in brown dwarfs has been particularly prominent in the interpretation of their spectral and photometric properties. Theory has been led in unexpected directions by unpredicted behaviors: the very strong evolution of spectral type with age (Burrows et al. 1997); the "hump" in the J band magnitude as a function of spectral type at the L/T transition (Tinney et al. 2003); notable differences between infrared spectra of optically classified objects and vice-versa (e.g. fig 3 in Kirkpatrick 2008); a turnaround in color at the T8/T9 spectral type (Warren et al. 2007). We are also slowly uncovering significant numbers of L and T sub-dwarfs (Sivarani et al. 2009; Burgasser 2004; Bowler et al. 2009, 2010) and other peculiar objects that challenge the theoretical models.

Parallax is a crucial parameter for understanding these objects as it is the only direct way to calculate an absolute magnitude and hence energetic output. In brown dwarf structure models, particularly for T dwarfs, the determination of metallicity and surface gravity from spectra is degenerate (Leggett et al. 2009) and hence luminosity, which requires a parallax, is used to constrain either the radius or the temperature and help break this degeneracy. Precise absolute velocities, that in turn provide age and origin indications, require precise parallaxes.

In light of the role of distance it is important that for these new objects we have a significant sample with measured parallaxes. As shown in Figure 1, only a small fraction of known L/T dwarfs have measured parallaxes - the black histogram - which limits any calibrations and generalizations we can make. To increase the current sample the Osservatorio Astronomico of Turin and Observatório Nacional of Brazil begin in 2007 the PARarallaxes of Southern Extremely Cool objects (hereafter PARSEC) program to determine parallaxes for 140 bright L and T dwarfs. In Figure 1 we include the PARSEC objects that illustrate our goal to attain at least 10 objects per spectral bin for L dwarfs and to increase the current sample for the fainter T dwarfs. A number of other programs are also underway to address this shortfall (for example C. G. Tinney private communication and J. K. Faherty as part of the Brown Dwarf Kinematics Project (Faherty et al. 2009)) but even including the expected additional objects the results of the PARSEC program will at least double number of L and bright T dwarfs with parallaxes.

In this paper we present the PARSEC program: section 2 describes the instrument and target selection; section 3 details the observational and reduction procedures, and section 4 the procedures used to produce a catalog of standard proper motions and preliminary parallax solutions for 10 objects. Finally in section 5 we discuss some uses we have made of this catalog and future plans.

2. The PARSEC observational program

2.1. The instrument

The primary instrument for this program is the Wide Field Imager (WFI, Baade et al. 1999) on the ESO 2.2m telescope. This is a mosaic of 8 EEV CCD44 chips with 2k×4k 15 μm pixels, providing a total field of 32.5 by 32.5 arcmin. This instrument/telescope combination was chosen for a number of reasons:

1. The instrument is fixed and stable, both crucial requirements in relative astrometry work

2. The plate scale of 0.2"/pixel is optimal for

Brasil

[9]Instituto de Astronomia, Geofsica e Cincias Atmosfricas, Universidade de So Paulo, Rua do Mato, 1226 - Cidade Universitria, 05508-900 So Paulo - SP, Brazil

this work as it offers better than Nyquist sampling even in the best seeing.

3. The field size of 0.3 square degrees allows a reasonably thorough search for nearby companions

4. It already has a proven track record for the determination of parallaxes of dwarf objects (Ducourant et al. 2007)

It was decided to observe in the z band (Z+/61 ESO#846, central wavelength 964.8nm, FWHM 61.6nm) which was a compromise between the optimal QE of the system in the I band, and the expected brightness of the targets which have a $I-z$ of about 2. To keep the exposure times within 300s we observed only objects brighter than z <19.

2.2. Observations

The observational procedure is as follows.

1. For each field we make one quick 50s exposure and locate the target.

2. Using the WFI move-to-pixel procedure we offset the telescope to move the target to pixel (3400,3500), which is in a flat part of CCD#7 (Priscilla) at less than 1/4 of the diagonal leading to the optical center of the mosaic.

3. We make the first science exposure of 150s for objects with z <18.0 and 300s for z ≥18.0.

4. The camera is then slightly offset, 24 pixels in both directions, and the second science image of the same exposure time is automatically begun.

5. We check the counts of the target in the first image. If the signal-to-noise of the target in the first image is less than 100, in real time we increased the exposure time accordingly. This is usually only the case in particularly poor sky conditions.

This procedure is very efficient and the dead-time for the telescope is minimal. The total time for a target is 10-25 minutes depending on magnitude and other overheads, enabling us to observe 3-4 objects per hour. Our time allocation usually results in always having grouped nights and, as multiple observations in the same run are of limited value, to both increase the sample and allow some redundancy, the target list has 6-8 objects per hour. We attempted to observe the majority of targets close to the meridian except during the twilight hours when we wish to include rising or setting targets at their maximum parallactic factor.

Observations began in April 2007 and, as of September 2009, targets have between 1.5 and 2.5 years of observations. The frequency of observations have been reasonably constant with a 2-3 night run every two months.

Figure 2 displays the sky distribution of the targets. Table 1 summarizes the dates and nights of the observations taken up 2009.

Table 1: Observations of the PARSEC program at the ESO2p2/WFI up to 2009.

Date	Nights
April 2007	09, 10, 11, 12
August 2007	31
September 2007	01, 02
October 2007	05, 06, 07
January 2008	04, 05
February 2008	26, 27
April 2008	02, 03
May 2008	27, 28
August 2008	21, 22
October 2008	24, 26
December 2008	18, 20
March 2009	01, 02, 03
April 2009	30
May 2009	06, 08
July 2009	21, 22, 23
December 2009	15, 18, 21

2.3. Target Selection

The targets were selected using the following criteria:

1. All southern L and T dwarfs discovered before April 2007

2. Brighter than z=19

3. No more than 8 objects in any RA hour

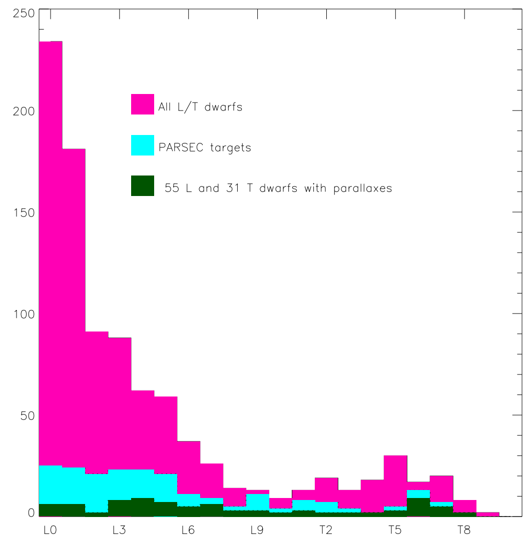

Fig. 1.— The distribution of the 752 known L and T dwarfs as of 2/2010 (www.dwarfarchives.org). Overplotted the distribution of the 90 objects with published parallaxes and the 140 objects in the PARSEC program as indicated in the legend.

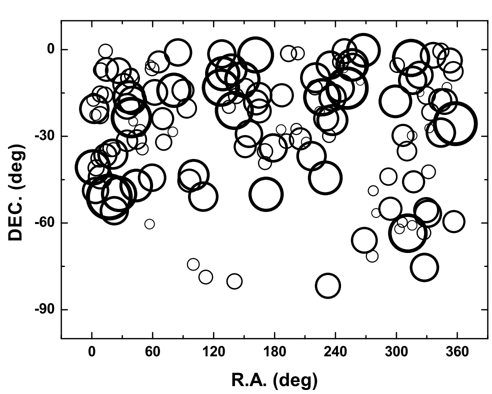

Fig. 2.— The equatorial coordinates distribution of the 140 sources of program. The size of the circles is in proportion to the object z magnitude. Notice that all targets belong in the austral hemisphere, and that they are clear of the galactic disk.

4. The brightest examples within each spectral bin

5. A uniform spectral class distribution

6. A photometric distance smaller than 50pcs.

The photometric distances were estimated using the 2MASS magnitudes transformed to the MKO system using Stephens & Leggett (2004) and the color - absolute magnitude compilation given in Knapp et al. (2004). Exceptions were made to include any objects that were underrepresented, e.g. most known T dwarfs are too faint for this program so any T dwarf with z $<$ 19 was given high priority. By applying the above criteria and by removing those objects we were not able to observe during the first runs due to time compression, the remaining list has 140 targets as shown in table 2. Listed are: the 2MASS counterpart name, shortened name used in this paper, published z-band magnitude - if no published value is available this is estimated from the J band magnitude and spectral type, 2MASS magnitudes, nominal spectral type and the discovery name. Most of the objects were chosen from the dwarfarchives.org while some are from the catalogs of Deacon & Hambly (2007) and Pokorny et al. (2004).

2.4. Image Reduction Procedures

The bias, dark and flat image corrections followed standard procedures while fringe removal required a tailored approach. The interference fringes in the WFI z-band image are severe, an examination of the counts shows they can vary by up to 10% over the distance of a few pixels. Fringing is an additive effect that can be corrected making a fringe map and subtracting it from the raw images. The suggested WFI approach is to apply a standard fringe map which is updated at periodic intervals. We found it improved our centroiding by adopting a different approach and to understand why we first consider the cause of fringing.

Fringes are caused by the constructive and destructive interference of the night sky emission lines that are reflected from the bottom of the CCD silicon layer with incoming radiation. Fringes are time and observation dependent for a number of reasons e.g.: changes in the brightness of the night sky emission lines, changes in the thickness of the silicon layer which is a function of the temperature of the CCD, changes in the angle of incidence of the light on the CCD which is a function of flexure. The ideal case would therefore be to make a fringe map for each image but this is not feasible. Our compromise is to make a nightly fringe map whenever possible.

The general procedure to construct a fringe map is to mask out objects then build a mean map from all of the observations in a given night scaled appropriately to reveal the fringe signal. Specifically we followed the following steps:

1. For all images we identify all the objects and make an object mask.

2. For each image we make a sky map by fitting a plane to all the unmasked pixels including a 3σ clipping rejection criteria. This changes in the course of the night so it is necessary to remove it from each frame independently.

3. We select a fringe calibration image subset consisting of all the short 50s and 4 of the long science exposures. We did not include all the science images in this subset as the object mask does not always cleanly block out all of the target signal and using all the science frames with the target on the same pixel results in a ghost image around the move-to-pixel position.

4. We make a median image by scaling all subset images by the exposure time and making a median of the unmasked pixels.

5. The first fringe map is constructed by smoothing the median image using a block size of 5 pixels.

6. This first fringe is subtracted from all images providing sky subtracted and relatively fringe free observations.

7. We make a new median image scaling the cleaned subset images by the weighted mean difference between the input image and the fringe image.

8. We construct a new fringe map smoothing the median image and then apply it to all the cleaned images providing fringe-free images.

In the first iteration we use the exposure time as a scale factor as the fringing will systematically affect the mean image counts, in the second the majority of the fringes are removed and we use the mean count as the scale factor which reflects the overall sky conditions as well. Below we discuss the effect of this fringing on the centroiding.

2.5. Centroiding and Feasibility Tests

The WFI, having a large field of view, has significant astrometric distortions and the CCDs have significant relative tilts (see the WFI section at www.eso.org). However, the fundamental requirements for relative astrometry, that underlie **all** small field parallax determinations, are stability and repeatability. For this reason we use the WFI move-to-pixel routine to put the target on the same pixel for each science exposure and only consider astrometric distortion changes over the observational campaign. The move-to-pixel position, (3400,3500), is sufficiently inside CCD#7 that reference stars from only the top third of the chip are needed to make a low-noise astrometric transformation between different epochs. The move-to-pixel procedure introduces a significant overhead but as shown by Platais et al. (2002), on a similar mosaic, the chips move relative to one another and this introduces a change in the astrometric deformation that was impossible to model at the mas level as required by our parallax goal.

We have tested three centroiding routines: a two dimensional Gaussian fit to the psf as used in the Torino Observatory Parallax Program (Smart et al. 1999, TOPP), a one-dimensional Gaussian fit to the marginal distributions, and the Gaussian psf fit provided by daophot in IRAF. In a comparison of object positions observed on 14 nights over an 18-month period of the field around the object 0719-50 we found the TOPP routine worked best. In figure 3 we plot rms of the position differences as a function of instrumental z magnitude for the frames in question. The median rms for all objects is 23mas and for the brighter objects from 12-16 is 10mas. If we apply the same test on images that have not been fringe-corrected as described above we find the median precision has deteriorated to 28mas. Applying the fringe map supplied by the WFI calibration team provided a precision that was intermediate between a nightly fringe correction and no correction.

3. Parallaxes

To determine parallaxes for our targets we consider only the top third of CCD#7. This is sufficiently large that, at these magnitudes, we have enough reference objects for a transformation to a common system and sufficiently small we can assume the variation in astrometric distortion over the observational campaign is smaller than the errors of a linear transformation. Once the (x,y) coordinates have been determined, the parallax and proper motions are derived using the methods adopted in TOPP (Smart et al. 2003, 2007). Schematically, we transfer the base frame to a standard coordinate system using the UCAC2 stars, adjust all subsequent frames to this base frame using all common stars and a simple linear transformation, and find the relative parallax and proper motion of the target star by a fit to the resulting observations in the system of the base frame. In the z-band the atmospheric refraction is small and we assume the differential color refraction to be negligible (Stone 2002). To calculate the correction from relative to absolute parallax we use the galaxy model of Mendez & van Altena (1996) in the z band to estimate the mean distance of the common stars. For the reference stars in these fields this parallactic mean distance is of the order of 1mas with an error of $<30\%$. For more details on the parallax determination procedure and this correction the reader is refered to Smart et al. (2003, 2007).

In figure 4 we reproduce the solutions for two targets, 0719-50 and 1004-33. These two objects were also found to have companions as discussed below. In Table 3 we report the parallaxes for 10 objects observed in the early runs of the PARSEC program. Listed are: object ID, position, number of stars, number of frames, absolute parallax, absolute proper motions, epoch difference and correction applied from relative to absolute parallax. In the following we discuss some of these objects in more detail.

0539-00 This object was found to have a photometric variability on a timescale of 13.3h (Bailer-Jones & Mundt 2001), we note in our sequence the instrumental magnitude decreases by 0.05±0.03 magnitudes over the two year sequence. The radial velocity was found not to vary for two observations spaced 4 years, excluding a companion of mass greater than 10 M_J (Zapatero Osorio et al. 2007); the astrometric residuals also show no evidence for binarity.

0719-50 For this object we find μ_α, μ_δ = 198.1 ± 3.2, -61.4 ± 3.9 mas/yr and it is identified by the PARSEC observations as a common proper motion companion of 2MASS07193535-5050523 with μ_α, μ_δ = (200.3 ± 8.9, -67.6 ± 5.7). The parallaxes both agree within the errors confirming the binary nature of this system. Both these objects have previous proper motion estimates, 0719-05 of 199.11 ± 20.49, -46.440 ±13.78 mas/yr (Casewell et al. 2008) and 2MASS07193535-5050523 of 206.2,-64.2 (Finch et al. 2007), but they were not noted as a common proper motion system. The analysis of the proper motion distributions in the range of magnitude and in the sky loci surveyed by the entire PARSEC program, gives a probability smaller than 0.002 for a chance occurance of such common pair of large proper motions. This chance becomes even smaller if the common distance is also considered. The brighter star has GSC2.3 magnitudes of B_J =16.01, R_f =13.50 and I_n=11.60 and 2MASS magnitudes of J=10.33, H=9.74, and K= 9.482. Combining the magnitudes and distance with the calibrations in Hawley et al. (2002) we find that the most consistent spectral type for this object is a M3-M4 dwarf.

0835-08 Cruz et al. (2003) find a spectroscopic distance of 8.3pc in agreement with our distance of 8.5pc, the nearest target in this sample and one of nearest known L dwarfs to date. The astrometric residuals present no evidence of binarity, which, combined with the consistency of the photometric and parallactic distances, allows us to confidently say that this is a single system.

0909-06 This is considered the prototypical L0 object, marking the begining of the L dwarf sequence with a temperature of 2200K (Basri et al. 2000). We expect by the end of the program to have the distance to this object to better than 5%.

1004-33 We confirm, as suggested in Casewell et al. (2008) and Seifahrt et al. (2005), that this object is a binary companion of the nearby bright object LHS5166. The proper motions and parallaxes of the two objects are both within one sigma of each other. The brighter star has GSC2.3 magnitudes of B_J =15.51, R_f =13.33 and I_n=11.29 and 2MASS magnitudes of J=9.85, H=9.30, and K=9.03. Combining the magnitudes and distance

Table 3: Parallaxes and proper motions for a sample of PARSEC L-dwarfs.

ID	α h:m:s	δ d:':"	N_*, N_f	π mas	μ_α mas/yr	μ_δ mas/yr	ΔT yrs	COR mas
0539-00	5:39:51.9	- 0:58:58.3	31, 12	82.0 ± 3.1	157.0 ± 4.8	321.6 ± 3.9	1.40	1.13
0641-43	6:41:18.5	-43:22:28.0	14, 29	55.7 ± 5.7	215.9 ± 8.9	612.8 ± 9.0	1.95	1.00
0719-50	7:19:32.0	-50:51:41.3	22, 34	32.6 ± 2.4	198.1 ± 3.2	-61.4 ± 3.9	1.98	0.90
0835-08	8:35:42.2	- 8:19:21.7	9, 20	117.3 ± 11.2	-519.8 ± 7.7	285.4 ± 10.5	1.96	1.08
0909-06	9:09:57.3	- 6:58:18.8	20, 23	42.5 ± 4.2	-184.0 ± 2.5	20.7 ± 3.0	2.08	1.19
1004-33	10:04:39.5	-33:35:21.9	16, 22	54.8 ± 5.6	243.5 ± 4.0	-253.2 ± 3.4	2.06	9.51
1018-29	10:18:58.5	-29:09:54.2	32, 23	35.3 ± 3.2	-340.8 ± 1.8	-94.0 ± 2.7	2.08	1.01
1539-05	15:39:42.1	- 5:20:41.5	17, 18	64.5 ± 3.4	603.1 ± 2.6	105.0 ± 3.4	2.06	1.12
1705-05	17:05:48.4	- 5:16:46.9	96, 17	44.5 ± 12.0	110.9 ± 12.1	-115.5 ± 7.1	1.98	0.59
1750-00	17:50:24.5	- 0:16:13.6	29, 39	108.5 ± 2.6	-398.3 ± 3.1	195.3 ± 3.4	2.08	0.56

NOTE.—N_* = number of reference stars, N_f = number of frames, ΔT = epoch range, COR = correction to absolute parallax.

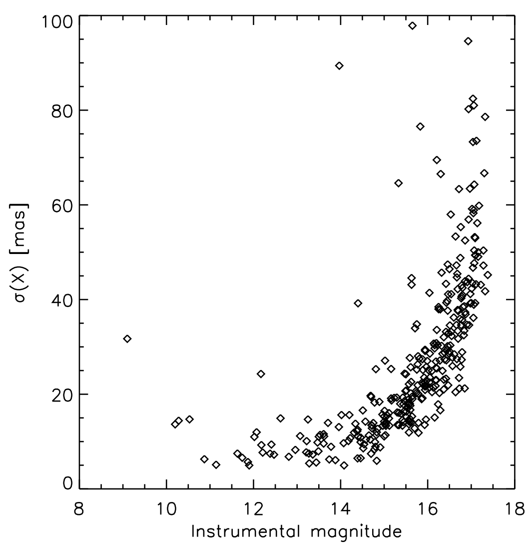

Fig. 3.— The root-mean-square of the X coordinates residuals for stars in common with a 0719-50 image sequence spanning 1.5 years as a function of z magnitude. The centroids were all derived using the TOPP two dimensional gaussian fit.

with the calibrations in Hawley et al. (2002) we find the spectral type for this object is a M3 dwarf consistent with the dM4.5e found in Seifahrt et al. (2005).

1705-05 In Reid et al. (2006) they consider the possibility that this object is part of a binary system with a companion at position angle of 5° and distance 1".36. This proposed companion was too faint to be frequently observed as part of our program, however, the color indicates a spectral type of T1-T2 that is inconsistent with the spectral type indicated by the apparent magnitude and distance of T7-T9. Hence, we conclude this object is more likely to be a background late M dwarf at ~200 parsecs rather than a companion to 1705-05.

1750-00 Based on spectroscopic observations, Kendall et al. (2007) found a distances of $8^{+0.9}_{-0.8}$pc and due to a discrepancies in the spectral type indicators suggest that it may be a binary system of L5-L6 and L8-L9 dwarfs. We find the trigonometric distance is consistent with the photometric one and do not find any evidence of binarity in the residuals which implies it is a single system and the discrepancies must have some other explanation.

0641-43, 1018-29 & *1539-05* The first two objects are type L1, and the third is L2. They are all in the 20-30pc distance range. 0641-43 and 1539-

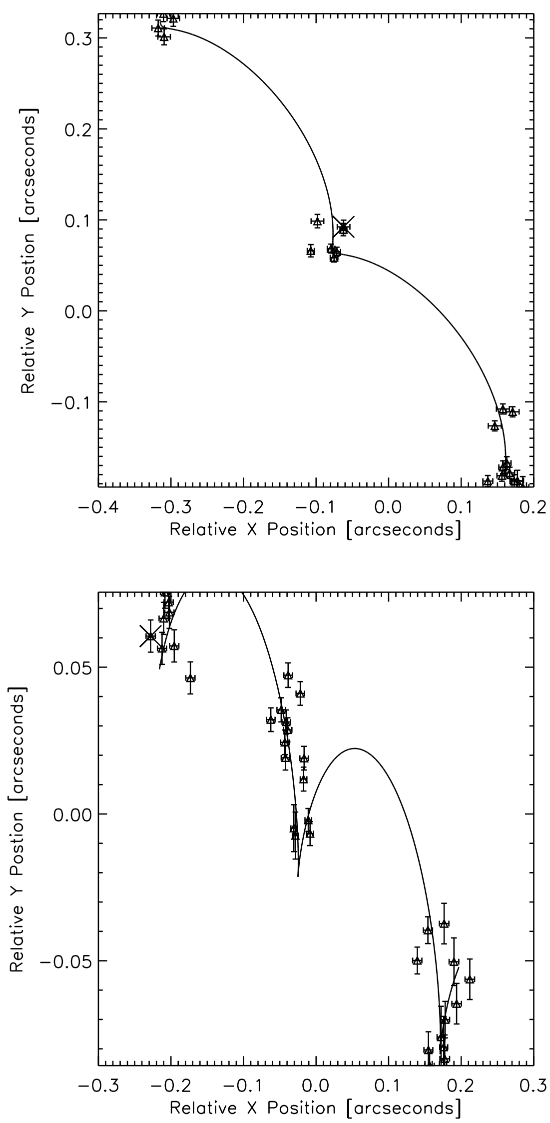

Fig. 4.— Observations for two example targets 0719-50 and 1004-33.

05 are fast moving objects, with one of the proper motion components larger than 600mas/yr. None of them was the subject of any particular discussion in the literature.

Figure 5 compares the trigonometric parallaxes from Table 3 against the corresponding spectroscopic parallaxes based on the calibration of Knapp et al. (2004). The small number of sources precludes any direct conclusion, yet the targets asymmetry relatively to the equal values diagonal brings support to the importance of trigonometric parallaxes as the fundamental calibrators for spectroscopic distances.

4. Proper Motions

The parallax determination of the targets uses only the upper third of CCD7; however, the reduction pipeline is applied to the entire mosaic of 8 CCDs. From this data we have constructed a proper motion catalogue, sampling the whole of the southern hemisphere with the exception of the lowest galactic latitudes where the number of known L/T dwarfs is significantly reduced. This proper motion survey can be used to search for companions to the targets, and other fast moving objects which will usually be nearby and/or sub-dwarfs. Combined with the magnitudes, the proper motion survey can also be used to build a reduced proper motion diagram to search for brown dwarf candidates. This catalog contains proper motion determinations for 195,700 objects.

Independently for each CCD and each observation we have determined an astrometric reduction relative to the Second US Naval Observatory CCD Astrograph Catalog (UCAC2, Zacharias et al. 2004). The average number of reference stars was 20, with which polynomial functions were adjusted on right ascension and declination. Depending on the number of reference stars the polynomial degree was 2 or 3 and cross terms have been included. The rms errors of the solutions did not show any dependence on the type of polynomial employed.

The proper motion determination was made from a match to the 2MASS point source catalogue. In principle, the program frames should be complete with respect to 2MASS and the epoch difference is small, so a nearest neighbor match should be sufficient to not mismatch high proper motion objects. As a safety measure, the proper

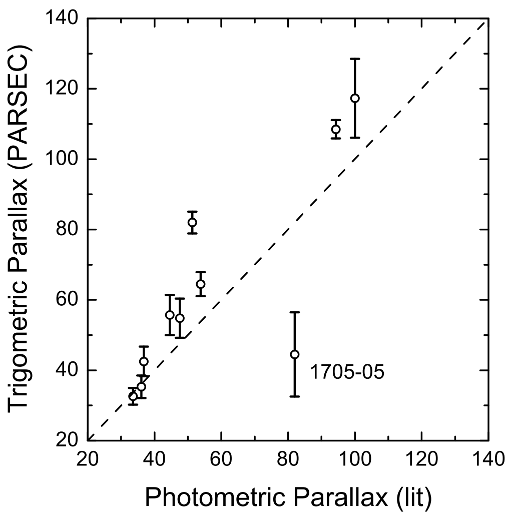

Fig. 5.— Comparison between the preliminary parallaxes derived by the PARSEC program for the 10 targets in Table 3 against the corresponding spectroscopic parallaxes. Notice how the photometric parallax of 1705-05 is affected by the superimposed nearby star (see text).

motions were determined for each observation combination and later averaged. Deviant values were removed from these averages, as they either came from unrecognised frame defects or faulty measurements. A more robust algorithm is being developed using the GSC2.3 positions at different epochs. At the targets galactic latitudes, blending is rare and its effects would be negligible to the relatively bright 2MASS stars.

The histograms of the right ascension and declination proper motions distributions are presented in Figure 6. The mean value for α is -2.8mas/yr (standard deviation σ=12.1mas), and -4.0mas/yr (standard deviation σ=12.3mas) for δ. This compares well with the corresponding values for the UCAC2 catalogue in the same regions, which are, -2.7mas/yr (standard deviation σ=14.6mas) for α, and -3.6mas/yr (standard deviation σ=30.1mas) for δ. Zonal averages ($3^h \times 30°$) also produced similar means for the PARSEC program and the UCAC2 catalogue stars. Figure 7 compares the proper motions of stars in common with the PARSEC program and the UCAC2 catalogue. The Pearson's linear correlation coefficient is 0.95 both on right ascension and on declination. The largest difference appear for the smallest proper motions (25mas/yr), the central parts in figure 7, where the PARSEC values typically exceed those from the UCAC2 by 6%.

Figure 8 is a similar comparison of the program target proper motions against values found in the literature. The linear correlation is 0.82. There are 5 outliers: 0523-14, 0559-14, 0624-45, 1828-48, and 1956-17. For each of the outliers a local comparison against the UCAC2 proper motions within the target's CCD have shown the same level of agreement found for the program as a whole. In the case of 0523-14 and 0624-45 the original proper motion paper (Schmidt et al. 2007) does not have any special discussion of these sources. Our results come respectively from 2 and 3 PARSEC observations, and more data must be added on to reach a clearer understanding. For 0559-14, the original proper motion paper (Dahn et al. 2002) indicates that the proper motion was taken within just 2.1 years, and the results should be taken as preliminary. For 1828-48 the original proper motion paper (Burgasser et al. 2004) indicates troublesome observations at high air mass and under patchy skies. For 1956-17 the original proper mo-

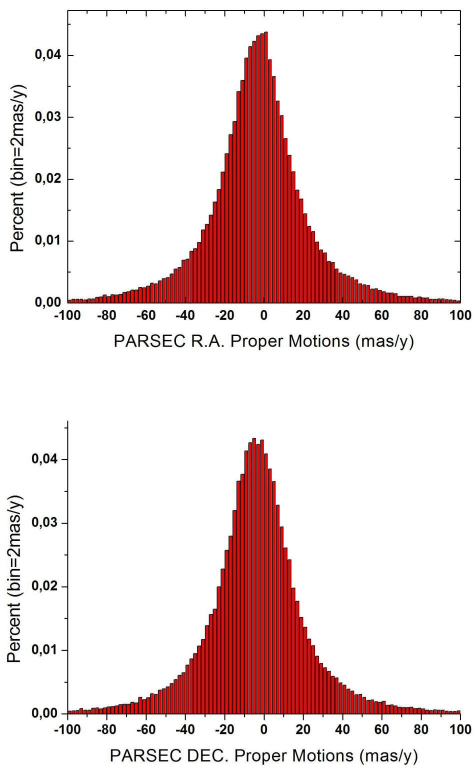

Fig. 6.— Proper motion distributions in right ascension and declination.

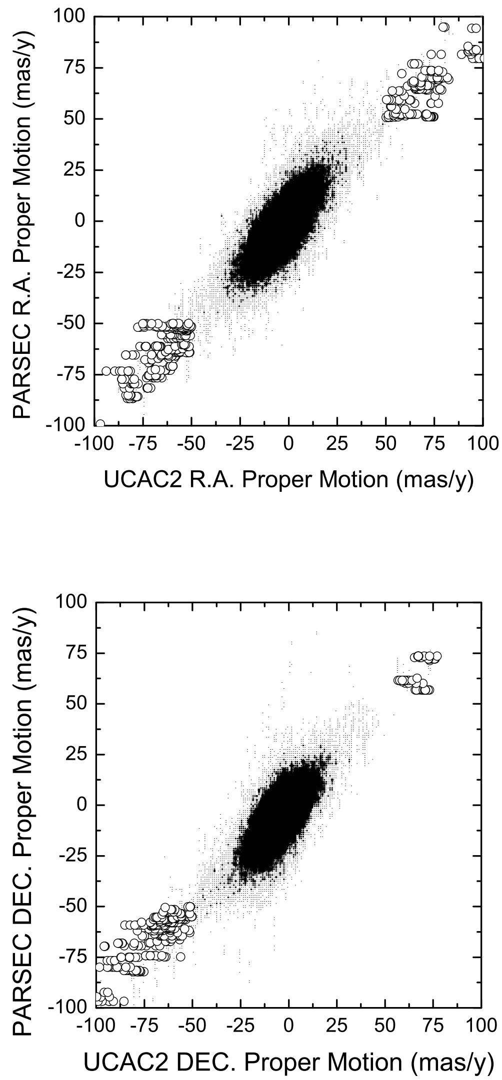

Fig. 7.— Comparison to UCAC2 proper motions in Right Ascension top panel and in Declination lower panel. For the smaller proper motions, the pairs in bins of 1mas/y are represented by dots with sizes proportional to the counts in the bin. The pairs in which any member is larger than |50|mas/y are individually represented by open circles.

tion paper is from the SuperCOSMOS Sky Survey (Hambly et al. 2001) which for individual objects may have large errors while our results include 7 consistent PARSEC observations.

The histograms of the proper motion errors are shown in Figure 9. The mean values are 5mas/yr both for right ascension and declination. The similarity of the behaviour in both coordinates, already seen in the comparison to UCAC2 values and for the errors distribution, is shown in Figure 10, where the pair-wise RA and DEC proper motions are plotted for all objects. The actual proper motions distribution reflects several factors, prominently the galactic rotation, and an uniform distrubution modulated by the inverse square of the distance. The combination of factors may result either in a Poisson-like or in a Gaussian-like distribution. We want to investigate whether the peculiar geometry of each CCD, and/or some artifact left by the astrometric reduction made indepently for each of them would reflect on the proper motions distribution. In order to not assume an a priori model, the cumulative density distribution of the proper motions was fitted by an exponential decay, either along the RA or the DEC directions, and indeed when those are quadratically combined to produce the apparent sky motion. The exponential decays are characterized by the one free parameter which we call scale length. It is an uncomplicated, robust estimator borrowed from the description of stochastic processes in which events can occur continuously and are independently of one another. We calculated the scale length in density steps of 10mas/yr in order to investigate the presence of clumps, voids, or systematics within the parent proper motions population. This was done for each CCD, as shown in Table 4. From one CCD to another the variation of the least-squares adjusted scale length was always smaller than the rms of the adjustments, implying consistent astrometric precision from the different CCDs.

The proper motion catalogue will be provided upon request ([1]). We have chosen not to distribute it to the data centers until the observations are finished and we have a final product. The above evaluation and our first release is based on the

[1] The preliminary catalog can be retrieved from the PARSEC web site at http://parsec.oato.inaf.it/data_releases.html

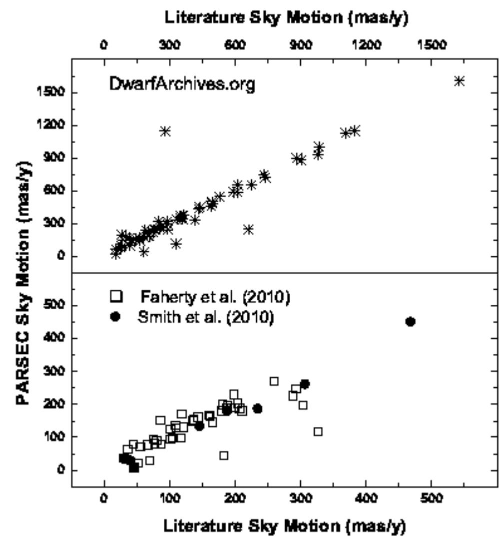

Fig. 8.— Comparison to literature values of the proper motions for the targets. On the top panel the comparison is made for the 58 PARSEC targets found in the archives of DwarfArchives.org. On the bottom panel the comparison is made for the most recent papers - 45 PARSEC targets in (Faherty et al 2010) and 8 PARSEC targets in (Schmidt et al. 2010b). Notice the different scale range in the two panels

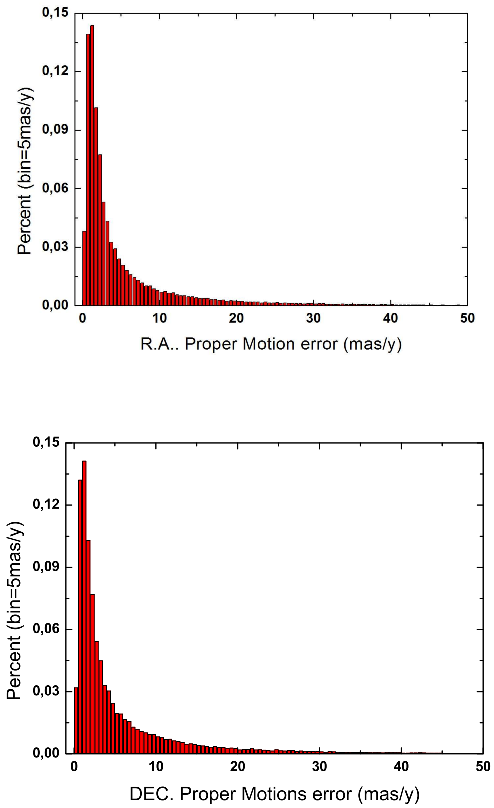

Fig. 9.— The distribution of the right ascension and declination proper motion errors.

Table 4: Scale length of the exponential decay of the separate and total proper motion distributions. Values are presented for all objects, and then by CCD.

CCD	Scale Length		
	Total +/- σ mas/yr	$\mu_\alpha \pm \sigma$ mas/yr	$\mu_\delta \pm \sigma$ mas/yr
ALL	34.3 $\pm$ 7.6	35.9 $\pm$ 8.0	34.4 $\pm$ 7.7
1	34.3 $\pm$ 7.6	35.9 $\pm$ 8.0	34.4 $\pm$ 7.7
2	30.7 $\pm$ 6.6	30.6 $\pm$ 7.1	29.0 $\pm$ 6.5
3	29.7 $\pm$ 6.3	29.6 $\pm$ 6.8	30.6 $\pm$ 6.7
4	35.9 $\pm$ 8.0	34.4 $\pm$ 7.7	34.1 $\pm$ 7.8
5	30.6 $\pm$ 7.1	29.0 $\pm$ 6.5	30.0 $\pm$ 6.9
6	29.6 $\pm$ 6.8	30.6 $\pm$ 6.7	26.6 $\pm$ 6.2
7	34.4 $\pm$ 7.7	34.1 $\pm$ 7.8	30.7 $\pm$ 7.3
8	29.0 $\pm$ 6.5	30.0 $\pm$ 6.9	27.0 $\pm$ 6.8

first year of the program, comprising 6 observation periods, from April/2007 up to April/2008.

In figure 11 we plot the reduced proper motion, $H(K) = K + 5 \times log(\mu_{tot}) + 5$, as a function of the $z - K$ color. The z magnitudes come from a zero point correction to the instrumental magnitudes of the first observations, the K are 2MASS magnitudes. The targets appear as white diamonds and they delineate the brown dwarf zone. The field stars are represented by contour levels, from a 100 $\times$ 100 matrix of stars count. From the field stars furthermost in the targets zone possible brown dwarf candidates can be identified for spectroscopic follow up.

5. Conclusion

We have presented the first parallaxes from the PARSEC program. The results bode well for the whole program which is expected to finish in early 2011. We have confirmed a candidate binary (1004-33) and discovered another (0719-50), both of which will make good benchmark systems. The WFI has a large field of view so we are able to put very good constraints on the wide binary systems and the parallaxes allow us to immediately isolate unresolved binaries because of their over luminosity with respect to their color. Given these two properties, and the large sample, we expect to be able to put sensible constraints on the binary frac-

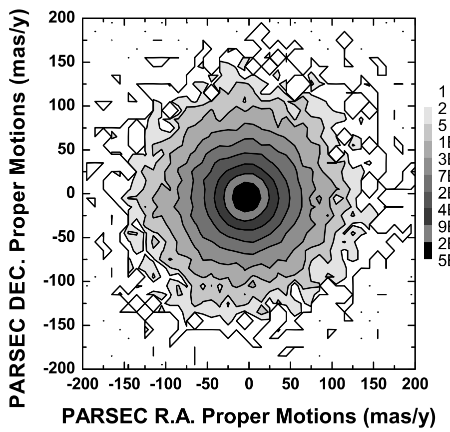

Fig. 10.— The right ascension vs declination proper motion contour plot for all the stars in the PARSEC fields.

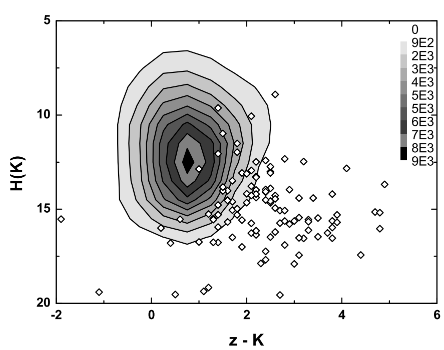

Fig. 11.— A reduced proper motion diagram of all objects in the PARSEC proper motion catalog. Diamonds are the targets and delineate the brown dwarf zone. The contour levels mark the quantity of field stars within the zone of the diagram. From the field stars furthermost in the targets zone possible brown dwarf candidates can be identified for spectroscopic follow up.

tion of brown dwarfs, a quantity that is critical for estimating the substellar mass function. We have produced a catalog of proper motions sampling the whole of the southern hemisphere. This catalogue provides an independent validation of the UCAC2 proper motion system. The proper motion distributions are shown to be statistically well behaved, it follows that the proper motions for the fainter objects will have the same precision. We will continue to update online this catalog until the end of the program and we plan to improve it including also GSC23 database observations.

6. Acknowledgments

The authors would like to acknowledge the support of: the Royal Society International Joint Project 2007/R3; the PARSEC International Incoming Fellowship and IPERCOOL International Research Staff Exchange Scheme within the Marie Curie 7th European Community Framework Programme. AHA thanks CNPq grant PQ-307126/2006-0. JIBC acknowledges CNPq financial support #477943/2007-1. DNSN thanks FAPERJ grant E-26/110.177/2009.

This research has made use of: the SIMBAD database operated at CDS France; the Second Guide Star Catalog developed as a collaboration between the Space Telescope Science Institute and the Osservatorio Astronomico di Torino; the Two Micron All Sky Survey which is a joint project of the University of Massachusetts and the Infrared Processing and Analysis Center/California Institute of Technology; and, the M, L, and T dwarf compendium housed at dwarfArchives.org and maintained by Chris Gelino, Davy Kirkpatrick, and Adam Burgasser.

REFERENCES

Baade, D., et al. 1999, The Messenger, 95, 15

Bailer-Jones, C. A. L., & Mundt, R. 2001, A&A, 367, 218

Basri, G., Mohanty, S., Allard, F., Hauschildt, P. H., Delfosse, X., Martín, E. L., Forveille, T., & Goldman, B. 2000, ApJ, 538, 363

Becklin, E. E., & Zuckerman, B. 1988, Nature, 336, 656

Bowler, B. P., Liu, M. C., & Cushing, M. C. 2009, ApJ, 706, 1114

Bowler, B. P., Liu, M. C., & Dupuy, T. J. 2010, ApJ, 710, 45

Burgasser, A. J. 2004, ApJ, 614, L73

Burgasser, A. J., McElwain, M. W., Kirkpatrick, J. D., Cruz, K. L., Tinney, C. G., & Reid, I. N. 2004, AJ, 127, 2856

Burrows, A., et al. 1997, ApJ, 491, 856

Casewell, S. L., Jameson, R. F., & Burleigh, M. R. 2008, MNRAS, 390, 1517

Cruz, K. L., Reid, I. N., Liebert, J., Kirkpatrick, J. D., & Lowrance, P. J. 2003, AJ, 126, 2421

Dahn, C. C., et al. 2002, AJ, 124, 1170

Deacon, N. R., & Hambly, N. C. 2007, A&A, 468, 163

Ducourant, C., Teixeira, R., Hambly, N. C., Oppenheimer, B. R., Hawkins, M. R. S., Rapaport, M., Modolo, J., & Lecampion, J. F. 2007, A&A, 470, 387

Epchtein, N., et al. 1999, A&A, 349, 236

Faherty, J. K., Burgasser, A. J., Cruz, K. L., Shara, M. M., Walter, F. M., & Gelino, C. R. 2009, AJ, 137, 1

Faherty, J. K., Burgasser, A. J., West, A. A., Bochanski, J. J., Cruz, K. L., Shara, M. M., & Walter, F. M. 2010, AJ, 139, 176

Finch, C. T., Henry, T. J., Subasavage, J. P., Jao, W., & Hambly, N. C. 2007, AJ, 133, 2898

Hambly, N. C., et al. 2001, MNRAS, 326, 1279

Hawley, S. L., et al. 2002, AJ, 123, 3409

Kendall, T. R., Jones, H. R. A., Pinfield, D. J., Pokorny, R. S., Folkes, S., Weights, D., Jenkins, J. S., & Mauron, N. 2007, MNRAS, 374, 445

Kirkpatrick, J. D. 2008, in Astronomical Society of the Pacific Conference Series, Vol. 384, 14th Cambridge Workshop on Cool Stars, Stellar Systems, and the Sun, ed. G. van Belle, 85–+

Kirkpatrick, J. D., et al. 1999, ApJ, 519, 802

Knapp, G. R., et al. 2004, AJ, 127, 3553

Leggett, S. K., et al. 2009, ArXiv e-prints

Mendez, R. A., & van Altena, W. F. 1996, AJ, 112, 655

Nakajima, T., Oppenheimer, B. R., Kulkarni, S. R., Golimowski, D. A., Matthews, K., & Durrance, S. T. 1995, Nature, 378, 463

Platais, I., et al. 2002, AJ, 124, 601

Pokorny, R. S., Jones, H. R. A., Hambly, N. C., & Pinfield, D. J. 2004, A&A, 421, 763

Reid, I. N., Lewitus, E., Allen, P. R., Cruz, K. L., & Burgasser, A. J. 2006, AJ, 132, 891

Schmidt, S. J., Cruz, K. L., Bongiorno, B. J., Liebert, J., & Reid, I. N. 2007, AJ, 133, 2258

Schmidt, S. J., West, A. A., Burgasser, A. J., Bochanski, J. J., & Hawley, S. L. 2010a, AJ, 139, 1045

Schmidt, S. J., West, A. A., Hawly, S. L., & Pineda, J. S. 2010b, AJ, 139, 1808

Seifhart, A., Mugrauer, M., Wiese, M., Neuhäuser, R., & Guenther, E, W. 2005, AN, 326, 974

Sivarani, T., Lépine, S., Kembhavi, A. K., & Gupchup, J. 2009, ApJ, 694, L140

Skrutskie, M. F., et al. 2006, AJ, 131, 1163

Smart, R. L., Bucciarelli, B., Lattanzi, M. G., Massone, G., & Chiumiento, G. 1999, Astron. Astrophys., 348, 653

Smart, R. L., Lattanzi, M. G., Jahreiß, H., Bucciarelli, B., & Massone, G. 2007, A&A, 464, 787

Smart, R. L., et al. 2003, A&A, 404, 317

Stephens, D. C., & Leggett, S. K. 2004, PASP, 116, 9

Stone, R. C. 2002, PASP, 114, 1070

Tinney, C. G., Burgasser, A. J., & Kirkpatrick, J. D. 2003, AJ, 126, 975

Warren, S. J., et al. 2007, MNRAS, 381, 1400

York, D. G., et al. 2000, AJ, 120, 1579

Zacharias, N., Urban, S. E., Zacharias, M. I., Wycoff, G. L., Hall, D. M., Monet, D. G., & Rafferty, T. J. 2004, AJ, 127, 3043

Zapatero Osorio, M. R., Martín, E. L., Béjar, V. J. S., Bouy, H., Deshpande, R., & Wainscoat, R. J. 2007, ApJ, 666, 1205

This 2-column preprint was prepared with the AAS LaTeX macros v5.2.

Table 2
PARSEC Targets as of 1/2009

2MASS ID	Red. ID	z	J	H	K_s	ST	Discovery ID
00043484-4044058	0004-40	15.8	13.109	12.055	11.396	L4.5	GJ 1001B, LHS 102B
00062050-1720506	0006-17	18.4	15.662	14.646	14.010	L2.5	2MASSI J0006205-172051
00100009-2031122	0010-20	16.5	14.134	13.368	12.882	L0.0	2MASS J00100009-2031122
00135779-2235200	0013-22	18.6	15.775	14.595	14.036	L4.0	2MASSI J0013578-223520
00145575-4844171	0014-48	16.8	14.050	13.107	12.723	L2.5	2MASS J00145575-4844171
00165953-4056541	0016-40	18.0	15.316	14.206	13.432	L3.5	2MASS J00165953-4056541
00300625-3739483	0030-37	17.9	15.204	14.426	13.885	L3.0	DENIS-P J003006.2-373948
00325584-4405058	0032-44	17.1	14.776	13.857	13.269	L0.0	EROS-MP J0032-4405
00324308-2237272	0032-22	17.9	15.388	14.512	13.962	L1.0	2MASSI J0032431-223727
00332386-1521309	0033-15	18.0	15.286	14.208	13.410	L4.0	2MASS J00332386-1521309
00345684-0706013	0034-07	18.2	15.531	14.566	13.942	L3.0	2MASSI J0034568-070601
00511078-1544169	0051-15	18.0	15.277	14.164	13.466	L3.5	2MASSW J0051107-154417
00531899-3631102	0053-36	17.2	14.445	13.480	12.937	L3.5	2MASS J00531899-3631102
00540655-0031018	0054-00	18.3	15.731	14.891	14.380	L1.0	SDSSp J005406.55-003101.8
00584253-0651239	0058-06	17.1	14.311	13.444	12.904	L0.0	SIPS0058-0651
01090150-5100494	0109-51	14.6	12.228	11.538	11.092	L1.0	SIPS0109-5100
01174748-3403258	0117-34	17.9	15.178	14.209	13.489	L2.0	2MASSI J0117474-340325
01230050-3610306	0123-36	16.4	13.639	13.108	12.191	L2.0	2MASSJ01230050-3610306
01253689-3435049	0125-34	18.3	15.522	14.474	13.898	L2.0	2MASSI J0125369-343505
01282664-5545343	0128-55	16.6	13.775	12.916	12.336	L2.0	SIPS0128-5545
01443536-0716142	0144-07	16.9	14.191	13.008	12.268	L5.0	2MASS J01443536-0716142
01473282-4954478	0147-49	15.8	13.058	12.366	11.916	L2.0[a]	...
02052940-1159296	0205-11	17.4	14.587	13.568	12.998	L5.5	DENIS-P J0205.4-1159
02182913-3133230	0218-31	17.4	14.728	13.808	13.154	L3.0	2MASSI J0218291-313322
02192807-1938416	0219-19	16.9	14.110	13.339	12.910	L2.5	SSSPM J0219-1939
02271036-1624479	0227-16	16.1	13.573	12.630	12.143	L1.0	2MASS J02271036-1624479
02304498-0953050	0230-09	17.7	14.818	13.912	13.403	T0.0[a]	...
02355993-2331205	0235-23	15.2	12.690	12.725	12.186	L1.0	GJ 1048B
02354756-0849198	0235-08	18.3	15.571	14.812	14.191	L2.0	SDSS J023547.56-084919.8
02394245-1735471	0239-17	16.6	14.291	13.525	13.039	L0.0	SIPS0239-1735
02431371-2453298	0243-24	18.9	15.381	15.137	15.216	T6.0	2MASSI J0243137-245329
02550357-4700509	0255-47	16.1	13.246	12.204	11.558	L9.0	DENIS-P J0255-4700
02572581-3105523	0257-31	17.6	14.672	13.518	12.876	L8.0	2MASS J02572581-3105523
03101401-2756452	0310-27	18.5	15.795	14.662	13.959	L5.0	2MASS J03101401-2756452
03185403-3421292	0318-34	18.5	15.569	14.346	13.507	L7.0	2MASS J03185403-3421292
03480772-6022270	0348-60	18.8	15.318	15.559	15.602	T7.0	2MASS J03480772-6022270
03504861-0518126	0350-05	18.8	16.327	15.525	15.125	L1.0	SDSS J035048.62-051812.8
03572695-4417305	0357-44	16.7	14.367	13.531	12.907	L0.0	DENIS-P J035726.9-441730
03572110-0641260	0357-06	18.3	15.953	15.060	14.599	L0.0	SDSS J035721.11-064126.0
04082905-1450334	0408-14	16.9	14.222	13.337	12.817	L4.5	2MASSI J0408290-145033
04234858-0414035	0423-04	17.3	14.465	13.463	12.929	L0.0	SDSSp J042348.57-041403.5

Table 2—*Continued*

2MASS ID	Red. ID	z	J	H	K_s	ST	Discovery ID
04390101-2353083	0439-23	17.3	14.408	13.409	12.816	L6.5	2MASSI J0439010-235308
04430581-3202090	0443-32	18.0	15.273	14.350	13.877	L5.0	2MASSI J0443058-320209
05185995-2828372	0518-28	18.8	15.978	14.830	14.162	L1.0	2MASS J05185995-2828372
05233822-1403022	0523-14	15.9	13.084	12.220	11.638	L5.0	2MASSI J0523382-140302
05395200-0059019	0539-00	16.7	14.033	13.104	12.527	L3.0	SIPS0539-0059
05591914-1404488	0559-14	17.3	13.802	13.679	13.577	T4.5	2MASS J05591914-1404488
06141196-2019181	0614-20	17.6	14.783	13.901	13.375	L4.0	SIPS0614-2019
06244595-4521548	0624-45	17.2	14.480	13.335	12.595	L5.0	2MASS J06244595-4521548
06395596-7418446	0639-74	18.5	15.795	14.723	14.038	L5.0	2MASS J06395596-7418446
06411840-4322329	0641-43	16.3	13.751	12.941	12.451	L1.5	2MASS J06411840-4322329
07193188-5051410	0719-50	16.5	14.094	13.282	12.773	L0.0	2MASS J07193188-5051410
07291084-7843358	0729-78	18.3	15.440	14.947	14.635	L0.0[b]	2_3367
08283419-1309198	0828-13	15.6	12.803	11.851	11.297	L2.0	SSSPM J0829-1309
08320451-0128360	0832-01	16.6	14.128	13.318	12.712	L1.5	2MASSW J0832045-012835
08354256-0819237	0835-08	15.9	13.169	11.938	11.136	L5.0	2MASSI J0835425-081923
08592547-1949268	0859-19	18.4	15.527	14.436	13.751	L6.0	2MASSI J0859254-194926
09095749-0658186	0909-06	16.2	13.890	13.090	12.539	L0.0	DENIS-P J0909-0658
09211410-2104446	0921-21	15.5	12.779	12.152	11.690	L4.5	2MASS J09211410-2104446
09221952-8010399	0922-80	18.1	15.276	14.285	13.681	L2.0	2MASS J09221952-8010399
09283972-1603128	0928-16	18.1	15.322	14.292	13.615	L2.0	2MASSW J0928397-160312
09532126-1014205	0953-10	15.8	13.469	12.644	12.142	L0.0	2MASS J09532126-1014205
10044030-1318186	1004-13	17.6	14.685	13.883	13.357	T0.0[a]	...
10043929-3335189	1004-33	17.3	14.480	13.490	12.924	L4.0	2MASSW J1004392-333518
10185879-2909535	1018-29	16.7	14.213	13.418	12.796	L1.0	2MASSW J1018588-290953
10452400-0149576	1045-01	15.7	13.160	12.352	11.780	L1.0	2MASSI J1045240-014957
10473109-1815574	1047-18	17.0	14.199	13.423	12.891	L2.5	DENIS-P J1047-1815
10584787-1548172	1058-15	16.9	14.155	13.226	12.532	L3.0	DENIS-P J1058.7-1548
10595138-2113082	1059-21	17.1	14.556	13.754	13.210	L1.0	2MASSI J1059513-211308
11220826-3512363	1122-35	18.1	15.019	14.358	14.383	T2.0	2MASS J11220826-3512363
11223624-3916054	1122-39	18.4	15.705	14.682	13.875	L3.0	2MASSW J1122362-391605
11263991-5003550	1126-50	15.9	13.997	13.284	12.829	L6.5	2MASS J11263991-5003550
11544223-3400390	1154-34	16.6	14.195	13.331	12.851	L0.0	2MASS J11544223-3400390
12255432-2739466	1225-27	18.8	15.260	15.098	15.073	T6.0	2MASS J12255432-2739466
12281523-1547342	1228-15	17.2	14.378	13.347	12.767	L6.0	DENIS-P J1228.2-1547
12462965-3139280	1246-31	18.2	15.024	14.186	13.974	T1.0[a]	...
12545393-0122474	1254-01	18.0	14.891	14.090	13.837	T2.0	SDSSp J125453.90-012247.4
13262009-2729370	1326-27	18.6	15.847	14.741	13.852	L5.0	2MASSW J1326201-272937
13314894-0116500	1331-01	18.4	15.459	14.475	14.073	L8.5	SDSS J133148.92-011651.4
13411160-3052505	1341-30	17.3	14.607	13.725	13.081	L2.0	2MASS J13411160-3052505
14044948-3159330	1404-31	18.8	15.577	14.955	14.538	T2.5	2MASS J14044941-3159329
14252798-3650229	1425-36	16.5	13.747	12.575	11.805	L5.0	DENIS-P J142527.97-365023.

Table 2—*Continued*

2MASS ID	Red. ID	z	J	H	K_s	ST	Discovery ID
14385498-1309103	1438-13	18.2	15.490	14.504	13.863	L3.0	2MASSW J1438549-130910
14413716-0945590	1441-09	16.4	14.020	13.190	12.661	L0.5	DENIS-P J1441-0945, G 124-6
14571496-2121477	1457-21	18.8	15.324	15.268	15.242	T7.5	Gliese 570D
15074769-1627386	1507-16	15.6	12.830	11.895	11.312	L5.5	2MASSW J1507476-162738
15200224-4422419	1520-44	16.0	13.228	12.364	11.894	L4.5	2MASS J15200224-4422419A
15230657-2347526	1523-23	17.0	14.203	13.420	12.903	L2.5	2MASS J15230657-2347526
15302867-8145375	1530-81	17.0	14.154	13.601	13.404	L0.0[b]	2_105
15344984-2952274	1534-29	18.4	14.900	14.866	14.843	T5.5	2MASSI J1534498-295227
15394189-0520428	1539-05	16.6	13.922	13.060	12.575	L2.0	DENIS-P J153941.96-052042.
15474719-2423493	1547-24	16.3	13.970	13.271	12.742	L0.0	DENIS-P J154747.2-242349
15485834-1636018	1548-16	16.7	13.891	13.104	12.635	L2.0	2MASS J15485834-1636018
16184503-1321297	1618-13	16.6	14.247	13.402	12.920	L0.0	2MASS J16184503-1321297
16202614-0416315	1620-04	18.0	15.283	14.348	13.598	L2.5	GJ 618.1B
16335933-0640552	1633-06	19.0	16.138	15.165	14.544	L6.0	SDSS J163359.23-064056.5
16360078-0034525	1636-00	17.0	14.590	13.904	13.415	L0.0	SDSSp J163600.79-003452.6
16452211-1319516	1645-13	15.0	12.451	11.685	11.145	L1.5	2MASSW J1645221-131951
17054834-0516462	1705-05	16.1	13.309	12.552	12.032	L4.0	DENIS-P J170548.38-051645.
17072343-0558249	1707-05	16.7	12.052	11.260	10.711	L3.0	2MASS J17072343-0558249B
17374334-1057425	1737-10	19.0	15.842	15.348	15.054	T2.0[a]	...
17502484-0016151	1750-00	16.0	13.294	12.411	11.849	L5.5	2MASS J17502484-0016151
17534518-6559559	1753-65	16.9	14.095	13.108	12.424	L4.0	2MASS J17534518-6559559
18244550-7128196	1824-71	18.5	15.677	15.290	14.849	L0.0[b]	2_5716
18283572-4849046	1828-48	18.7	15.175	14.908	15.181	T5.5	2MASS J18283572-4849046
18401904-5631138	1840-56	18.9	16.066	15.523	15.186	L9.0[b]	2_5580
19285196-4356256	1928-43	17.9	15.199	14.127	13.457	L4.0	2MASS J19285196-4356256
19360187-5502322	1936-55	17.2	14.486	13.628	13.046	L5.0	2MASS J19360187-5502322
19561542-1754252	1956-17	16.1	13.754	13.108	12.651	L0.0	2MASS J19561542-1754252
20025073-0521524	2002-05	18.2	15.316	14.278	13.417	L6.0	2MASS J20025073-0521524
20115649-6201127	2011-62	18.8	15.566	15.099	14.572	T1.0[a]	...
20232858-5946519	2023-59	18.7	15.530	14.965	14.485	T1.0[a]	...
20261584-2943124	2026-29	17.3	14.802	13.946	13.360	L1.0	2MASS J20261584-2943124
20414283-3506442	2041-35	17.6	14.887	13.987	13.401	L2.0	2MASS J20414283-3506442
20450238-6332066	2045-63	15.4	12.619	11.807	11.207	L4.0	SIPS2045-6332
20575409-0252302	2057-02	15.6	13.121	12.268	11.724	L1.5	2MASSI J2057540-025230
21015233-2944050	2101-29	18.8	15.604	14.845	14.554	T1.0[a]	...
21022212-6046181	2102-60	18.8	15.632	15.200	14.827	T2.0[a]	...
21041491-1037369	2104-10	16.6	13.841	12.975	12.369	L2.5	2MASSI J2104149-103736
21075409-4544064	2107-45	17.3	14.915	13.953	13.380	L0.0	2MASS J21075409-4544064
21304464-0845205	2130-08	16.7	14.137	13.334	12.815	L1.5	2MASSW J2130446-084520
21324898-1452544	2132-14	19.0	15.714	15.382	15.268	T3.0[a]	...
21481326-6323265	2148-63	18.3	15.330	14.338	13.768	L8.0[a]	...

Table 2—*Continued*

2MASS ID	Red. ID	z	J	H	K_s	ST	Discovery ID
21501592-7520367	2150-75	16.6	14.056	13.176	12.673	L1.0	2MASS J21501592-7520367
21574904-5534420	2157-55	17.0	14.263	13.440	13.002	L0.0	2MASS J21574904-5534420
21580457-1550098	2158-15	17.8	15.040	13.867	13.185	L4.0	2MASS J21580457-1550098
22041052-5646577	2204-56	16.7	11.908	11.306	11.208	T1.0	eps Indi Ba
22064498-4217208	2206-42	18.3	15.555	14.447	13.609	L2.0	2MASSW J2206450-421721
22092183-2711329	2209-27	18.9	15.786	15.138	15.097	T2,0[a]	...
22134491-2136079	2213-21	17.9	15.376	14.404	13.756	L0.0	2MASS J22134491-2136079
22244381-0158521	2224-01	16.9	14.073	12.818	12.022	L3.5	2MASSW J2224438-015852
22521073-1730134	2252-17	17.2	14.313	13.360	12.901	L7.5	DENIS-P J225210.73-173013.
22545194-2840253	2254-28	16.5	14.134	13.432	12.955	L0.5	2MASSI J2254519-284025
22552907-0034336	2255-00	18.0	15.650	14.756	14.437	L0.0	SDSSp J225529.09-003433.4
23101846-1759090	2310-17	16.9	14.376	13.578	12.969	L1.0	SSSPM J2310-1759
23185497-1301106	2318-13	18.8	15.553	15.237	15.024	T3,0[a]	...
23302258-0347189	2330-03	17.0	14.475	13.745	13.121	L1.0	2MASS J23302258-0347189
23440624-0733282	2344-07	17.6	14.802	13.846	13.232	L4.5	2MASS J23440624-0733282
23462656-5928426	2346-59	17.3	14.515	13.905	13.500	L5.0	SIPS2346-5928
23515044-2537367	2351-25	14.8	12.471	11.725	11.269	L0.0	SIPS J2351-2537

[a]These objects have been provided pre-publication from a study being undertaken by D. Pinfield (Univ. of Hertfordshire) of the Galactic Plane. The spectral types are based on photometry.

[b]These objects have been selected from the catalog of Pokorny et al. (2004) and photometrically classified.